

# Design and Control of a 3 DOF Hand Skeleton for Rehabilitation after Stroke

**M. Dehghani Rorani**

Department of Mechanical Engineering,  
Islamic Azad University, Majlesi Branch, Isfahan, Iran  
E-mail: valiasr\_mahdi@yahoo.com

**S. Rahmati\***

Department of Mechanical and Aerospace Engineering,  
Islamic Azad University, Science and Research Branch, Tehran, Iran  
E-mail: rahmati@rapidtoolpart.com

\*Corresponding author

Received: 6 December 2014, Revised: 30 December 2014, Accepted: 20 January 20154

**Abstract:** Stroke is one of the most common diseases among the elderly with high personal and societal costs. In recent years, robotic rehabilitation for stroke has become an active area of research for assistance, monitoring and qualifying the rehabilitation treatments. The key issue needed for improving rehabilitation system is that patient feedback should be taken into account by the robotic rehabilitation systems for providing rehabilitation treatment. Changes in the delivery of rehabilitation treatment are an important issue since the patient or specialist should be able to express their sense about doing things and apply the needed improvements in treatment. Therefore, in this study, a three degree-of-freedom (3-DOF) exoskeleton design of a thumb has been investigated. Then, a control structure is provided for greater security in which the patient feedback is evaluated in order to make necessary automatic changes in method of treatment (changing speed and force). In this design, a versatile framework with high performance is offered to simultaneously control thumb force and position regarding the patients' feedback. This may help to keep the patient in the treatment process, reduce interventions and therapist caseload, effective automatic transmission of treatment and pain relief during the course of treatment. The results of the study suggest that the force and speed on the thumb can be changed during the rehabilitation period according to the patient's needs. This advantage may be considered as an essential step for improvement of the rehabilitation efficiency.

**Keywords:** Patient Feedback, Thumb Exoskeleton, Thumb Force Control, Thumb Position Control

**Reference:** Dehghani Rorani, M., Rahmati, S., "Design and Control of a 3 DOF Hand Skeleton for Rehabilitation after Stroke", Int J of Advanced Design and Manufacturing Technology, Vol. 8/No. 2, 2015, pp. 17-28.

**Biographical notes:** **M. Dehghani Rorani** did his MSc in mechatronic engineering at IAU University, Majlesi Branch, Isfahan, Iran in 2015. His current research interest focuses on Biomedical instruments, Medical robots including biomechanics and bioelectric. **S. Rahmati** received his PhD in Advanced Manufacturing Technology from University of Nottingham, England, in 1999. He has also received his MSc and BSc from Loughborough University in UK and Ottawa University in Canada respectively. He is currently Associate Professor at the Department of Mechanical and Aerospace Engineering, Islamic Azad University, Science and Research Branch, Tehran, Iran. His current research interest includes Additive Manufacturing, Medical Rapid Prototyping, Advanced Manufacturing Processes and Rapid Tooling.

## 1 INTRODUCTION

Stroke is the most common and debilitating neurological injury in adults and it is the sudden onset of neurological symptoms due to cerebral blood supply impairment. According to the American Stroke Association statistics, one person suffers from stroke every 40 seconds [1]. Majority of people suffer from impaired arm function. Also, more than 40 per cent of these patients suffer from acute laxity on one side of the body which is an indicator of chronic Hemiparesis or chronic shortening of upper organs especially finger expansion [2].

Many studies have been conducted in recent years in order to treat these patients. The results of clinical studies have shown that Movement-based Therapy can significantly impact treatment of stroke patients. Hence, new methods have been created through adopting the Movement-based Therapy approach which deal with active training of affected organs to control the movements with organized and targeted behavioural tasks [3],[4]. “Shaping” method is one of the behavioural training methods conducted in accordance with the functions of organs which are used Constraint-Induced Movement therapy (CI) [5], [6]. This treatment provides optimum induction of the affected member in a quantitative, standardized and systematic format.

Access to such training methods is limited to various components including: a) Therapists ability for frequent, precise and controlled examination and evaluation of the arm and hand movements and b) Time allocated for each patient by therapists. The rehabilitation robots are used to automatize the specific training to plan and implement various levels of assistance to the patients regarding their progress during the rehabilitation period [7].

Finger disorder after stroke leads to a significant reduction in hand performance on daily tasks [8]. New advances in the field of Robotic rehabilitation are intended to improve the performance of the affected members. Although existing robotic systems may be able to provide a hardware device for arm rehabilitation, but so far, they have failed to provide this system for the fingers in practice. Moreover, there are several technical challenges like designing a specific system with independent control, power, speed and reliability for many of the finger joints. Moreover, the current devices lack sufficient precision for the purpose of human finger rehabilitation in terms of speed and torque.

Poli et al., proposed an exoskeleton robot with 3-DOF corresponding to up and down movements of hand, forearm and arm for rehabilitative purposes [9]. Dynamic modelling of the robot was based on Euler-Lagrange method. Robot dynamic parameters such as

weight, length and ligamentous laxity were determined based on the physical characteristic of an adult. Since the performance of such systems depends on the effects of force and pressure on human skeletal-muscle system occurring through the soft tissues, the impedance control method is used in the joint space. The simulation results indicated the high performance of the proposed robotic system for performing the rehabilitation movements suggested by the specialist [10].

Jamshidi et al., applied a bio-mechatronic approach to study the design and modelling of the robots that can strengthen the knee muscles. The robot had arms that intelligently increased knee muscle strength through involvement of the knee. The results indicated that this method can be used as a suitable method for the robot design and simulation for muscle rehabilitation [11].

Abdolvahab et al., showed that robotic rehabilitation methods providing high intensity practice of the affected members using Cognitive Processing Therapy (CPT) were more successful since the patients focused on preciseness of the process while performing repetitive movements. However, the patient may not be able to track and continue the desired movement due to difficulties during the implementation of the action. So, robotics assistant were used to help patients complete the exercises in different ways [12].

Worsnopp et al., designed an exoskeleton with three-degree-of-freedom to permit independent actuation of each of the three joints of the index finger to facilitate movement, especially of pinch (Figure 1). Separate actuators were used for flexion and extension, with closed-loop control of either force or position. This system was used to assess strategies for optimizing rehabilitation of pinch and reach-to-pinch following stroke. The evaluation results were promising for further research and study in the future [13].

Santos et al., stated that that different methods of rehabilitation for stroke patients which had been used until then included techniques based on Nero Developmental Training approaches which gradually led to of the patient's avoidance of daily activities. Stroke patients are usually trained to use compensatory strategies to perform daily activities instead of learning proper motor control along with the functional use of the affected members. Consequently, the rehabilitation intervention may be of some use to learning failure in these patients [14].

Abdollah et al., and Borgheasan et al., used Jason Taylor test to evaluate the effect using task-oriented training (TT) on the performance of upper limbs and showed that TT program improved the performance of hemiparetic stroke patients which positively affected primary sensorimotor cortex activities. [15],[16].

In this study a basic framework of intelligent control system is created for robots to assimilate the overall

control structure with the patient’s feedback. The main purpose of the present plan is to create a synchronous communication interface between the robotic system and the feedback system in order to develop supervisory control systems on different parts of the robot. The proposed robotic rehabilitation system changes the method of providing rehabilitation treatments based on the patient feedback.

## 2 MODELING

An exoskeleton of thumb was designed based on the characteristics of finger movement, and the mathematical equation governing the designed dynamic structure was extracted. An exoskeleton of thumb is designed to meet the following requirements: a) based on Mechanical point of view, it should be able to support the movement of the thumb across the moving spectrum and b) It should also be lightweight and generate the required force to the tip of the thumb to perform different movements including pinch or grabbing.

In addition to the limitation of motion, the exoskeleton should be a light-weighted structure so that the patient under rehabilitation would not feel it and the patient would not feel tired and uncomfortable due to the weight of the device. One of the most important aspects of the exoskeleton design was the ability to control the finger joints independently. As another important aspect of its design, the finger gestures should be configurable and have a wide range for rehabilitation. The skeleton should be offering all of the above.

Model of thumb motion is shown in Fig. 1 Flexion-Extension and the Adduction-Abduction have been described. The skeleton includes 5 Actuated Joints, 3 Passive Joints in order to achieve the independent control of each joint. All 8 joints are complex.

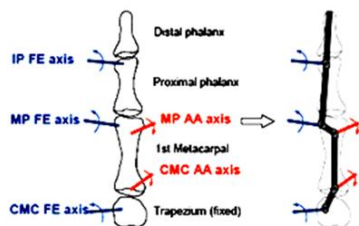


Fig. 1 Link model of the thumb [15]

Metatarsophalangeal joint (MCP), Carpometacarpal Joint (CMC), Interphalangeal Joint (IP), Flexion joint near CMC and Extension Joint near MPC are independently controlled. The exoskeleton is attached to the proximal and metacarpal of the thumb. The basic

point of movement in every part is connected to the previous part. Connection points are joined through two bars providing required length flexibility.

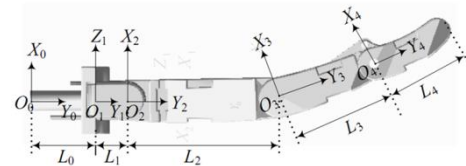


Fig. 2 Cartesian coordinate system in the thumb model

It is a big challenge to design a module for connecting exoskeleton to the thumb. Connector module is made of a basic plate attached to a fiberglass mould base wrapped in arm. To minimize the weight of the exoskeleton on patient's hand, the joints actuators are placed on a desk in a suitable gap joints on. Tendon (like a rope and pulley) is used to transmit the torque. These tendons can also transmit the rotary motion and also torque is transmitted from motors to the tendons. As the required torque varies according to different joints of the thumb, the corresponding pulleys have been also chosen differently. The smaller pulleys can transmit less torque but are lighter and have less inertia.

## 3 ALIGNING THE AXES OF THUMB AND THE EXOSKELETON AT CARPOMETACARPAL JOINT (CMC)

Flexion-Extension and adduction-Abduction axes in CMC are aligned from thumb to the exoskeleton. When the exoskeleton and thumb axes are aligned, movement of the thumb with two parallel links will have the same rotation axis. The advantage of such a design is to reduce the number of restricting connections to one. For example, two links are aligned while moving on a plan with their rotation axes, and if we want to write the constraint equation for the end of the tip, instead of writing the position equations for both links in x and y direction, one of the equations can be solved to satisfy each of the coordinate axes and other equation will be automatically satisfied.

So, for a two-dimensional system, constraint equations are reduced to one equation. Similarly, when a three-dimensional system is considered, only two constraint equations of (x,y) must be considered and the limitation in Z axis is satisfied automatically. This reduction of restriction is only applied for the primary contact point on metacarpal bone. Two remaining connected points of constraint equations needs to be solved for three directions. Therefore, in the end eight equations are used to compute eight unknowns. This is a unique practical configuration in which all the constraints are satisfied.

#### 4 HD PARAMETERS FOR EXOSKELETON

For all calculations and further modelling of exoskeleton, all DH parameters of the exoskeleton are measured. These parameters are listed in Table 1. In order to align the axes of exoskeleton and the thumb, DH parameters of the first three links were same as the Type II thumb [15].

**Table 1** HD parameters for Exoskeleton

i	$\eta_{i-1}$ (deg)	$L_{i-1}$ (mm)	$d_i$ (mm)	$i$ (rad) $\theta$
1	90	21	0	$\theta_v$
2	-90	9	0	$\theta_r$
3	0	45	0	$\theta_r$
4	0	30	0	0

Where,  $\eta_{i-1}$ : provides the rotation angle around the axis  $Y_{i-1}$ ,  $L_{i-1}$  is the distance between  $Z_{i-1}$  and  $Z_i$  and  $d_i$  is determined as distance between  $Y_{i-1}$  and  $Y_i$ .

#### 5 KINEMATIC ANALYSIS OF THUMB-EXOSKELETON SYSTEM

This section discusses the coupled motion of the thumb-exoskeleton system. The section broadly describes the forward and inverse kinematics routines followed by an open-loop control scheme for the thumb-exoskeleton system. In the open-loop control scheme, the thumb-tip is made to follow a desired trajectory, without violating the constraints (points of attachment of the thumb and the exoskeleton) in the system. The constraints and their mathematical formulation are also described in this section. For a finger with three-DOF, the fingertip's motion depends on the coupled link. A dynamic model of the finger with three-DOF can be described as follows [16]:

$$M(q)\ddot{q} + C(q, \dot{q})\dot{q} + g(q) = \tau - \tau_f + \tau_{ext} \quad (1)$$

Where  $M(q)$ ,  $C(q)$  and  $g(q)$  represent inertia matrix, centrifuge and gravity terms, respectively. Moreover,  $q$  represents the joint angle vector,  $\tau$  Joint torque vector,  $\tau_f$  friction torque vector and  $\tau_{ext}$  the external torque vector which is given by [17]:

$$\tau_{ext} = J^T F_t \quad (2)$$

Where  $J$  represents the Jacobian matrix and  $F_t = [F_x \ F_y \ F_z]^T$  indicates the thumb-tip force and  $\tau_m$  represents the motor torque vector. The  $\tau$ ,  $\tau_m$  relation is

shown as below: Firstly, for three-DOF finger, the transformation four tensions to three-joint torques is given by [18]:

$$\tau = Rf, \quad R = \begin{bmatrix} r_{11} & r_{12} & -r_{13} & -r_{14} \\ r_{21} & -r_{22} & r_{23} & -r_{24} \\ 0 & 0 & r_{33} & -r_{34} \end{bmatrix} \quad (3)$$

Where  $f$  represents the vector consisting of 4 tendon tensions,  $R$  represents the mapping from tendon tensions ( $f$ ) to joint torques ( $\tau$ ) and  $r_{ij}$  is the radius of a circular surface where the  $j$ -tendon envelops itself on the  $i$ -joint. therefore, for a 3-DOF finger,  $i=1,2,3$  and  $j=1,2,3,4$ . For thumb, we have:

$$\begin{aligned} r_{11} = r_{12} = r_{13} = r_{14} &= 5.5mm \\ r_{21} = r_{22} = r_{23} = r_{24} &= 5.2mm \\ r_{33} = r_{34} &= 5.0mm \end{aligned} \quad (4)$$

Secondly, the relationship between the tendon tensions and motor torques is expressed as:

$$f = \frac{2\pi}{d} \tau_m \quad (5)$$

Where  $d$  represents the screw pitch of the lead screws. According to equations (3) and (4), the equation (6) can be written as:

$$M(q)\ddot{q} + C(q, \dot{q})\dot{q} + g(q) = \frac{2\pi}{d} R \tau_m - \tau_f + \tau_{ext} \quad (6)$$

The above equation indicates that the tendons have an impact on the control of the tendon-driven robot hand. In order to simulate the performance of the tendons, the tendon model is built by adding bushing force between small stiffness cylinders. The force analysis between a two small cylinders is shown in Figure 3.

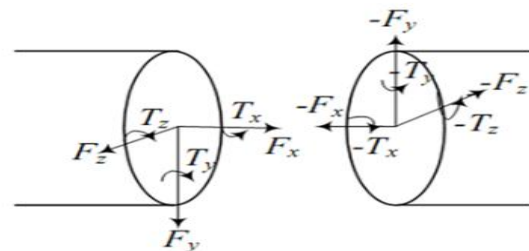


**Fig. 3** Tendon Force Analysis

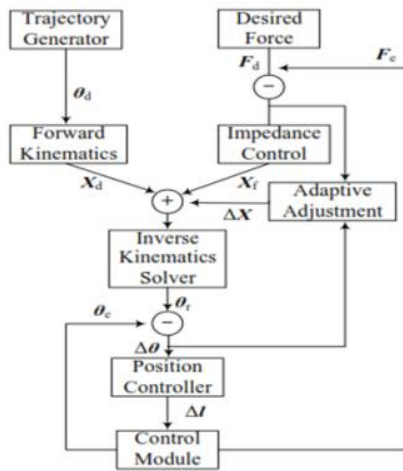


Fig. 4 Components of Control System

The dynamic equations of the tendon modelling can be expressed as:

$$\begin{bmatrix} F \\ T \end{bmatrix} = K \begin{bmatrix} R \\ \theta \end{bmatrix} - C \begin{bmatrix} V \\ \omega \end{bmatrix} + \begin{bmatrix} F_0 \\ T_0 \end{bmatrix} \quad (7)$$

$F_0$  and  $T_0$  are the initial values of the force and torque, respectively. In order to get a reasonable tendon model,  $K$  and  $C$  should be set to appropriate values. In the control of the robot hand, the tendons that are not flexible enough will affect the finger motion but the very flexible tendons will diminish the control accuracy. Considering that, the satisfying tendon models are built by adjusting the parameters of  $K$  and  $C$  in ref. [19]. The control system built for the three-DOF thumb consists of a control module, adaptive impedance controller, trajectory generator, inverse kinematics solver, position controller and other modules as shown in Fig. 4.

The trajectory generator provides the desired angular displacement  $\theta_d$ , which need to be converted to the desired displacement  $X_d$  in Cartesian-space by forward kinematics because the output of the adaptive impedance controller is in Cartesian-space. The adaptive impedance controller consists of an impedance control part and an adaptive adjustment part. The input of the impedance control part is the difference between the desired contact force  $F_d$  and the actual contact force  $F_e$  and the output is a displacement offset  $X_f$ .  $\Delta X$  is defined as the output of the adaptive adjustment part. Therefore, the displacement adjusted in Cartesian-space can be:

$$X_r = X_d + X_f + \Delta X \quad (8)$$

$X_r$  can be converted to the angular displacement  $\theta_r$  in joint-space by inverse kinematics.  $\Delta\theta$  represents the difference between  $\theta_r$  and the actual angular displacement  $\theta_e$ . The position controller can convert  $\Delta\theta$  to the tendon displacement offset  $\Delta l$ . The control module of three-DOF thumb is shown in the figure 4. The impedance control does not mean controlled position or force but rather it is the dynamic relation between the two [20]. The relation is an impedance equation, which is given by:

$$M_d(\ddot{X}_r - \ddot{X}_d) + B_d(\dot{X}_r - \dot{X}_d) + K_d(X_r - X_d) = E \quad (9)$$

Where  $E = F_d - F_e$  and  $M_d$ ,  $B_d$  and  $K_d$  are respectively  $3 \times 3$  constant-positive-diagonal matrices of the desired inertial, damping and stiffness. The impedance parameters of  $M_d$ ,  $B_d$  and  $K_d$  should keep the system in the critical damping state or overdamping state. An increasing  $M_d$  will result in a large impact to the environment. A large  $B_d$  can increase the response time with no vibration, where for position accurate tracking, a large  $K_d$  should be selected [39]. For a classical impedance control  $\Delta X = 0, X_f = X_r - X_d$ . So, Equation (7) can be expressed in the Laplace domain as follows [21]:

$$X_f(s) = \frac{E(s)}{M_d s^2 + B_d s + K_d} \quad (10)$$

According to Equation (10), the structure diagram of the impedance control compensator is shown in Fig. 5. However, the impedance control compensator is only suitable for a specific environment and the impedance parameters can't be changed in the whole control process. If the environmental parameters changed or weren't exact, the performance of the controller would be unsatisfactory. Hence, an adaptive adjustment is needed to change the impedance parameters indirectly according to the environment changes.

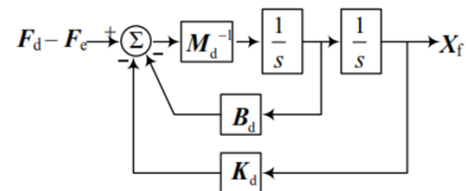


Fig. 5 Structure diagram of the impedance control compensator

The key of the adaptive adjustment is to get an adaptive offset  $\Delta X$  to compensate the output of the impedance control.  $\Delta x_k, f_{dk}, f_{ck}, x_{ck}, x_{dk}$  represent the  $K^{th}$  element of  $\Delta X, f_d, f_e, X_d$  ( $k= 1,2,3$ ). Then it can be expressed as:

$$\Delta x_k = g(t) + k_p(t)e(t) + k_d(t)\dot{e}(t) \quad (11)$$

Where  $g(t)$  is an auxiliary signal which contains the integral term.  $k_p(t)$  and  $k_d(t)$  are the adaptive proportional and derivative force feedback gain, respectively. Moreover,  $e(t) = f_{dk} - f_{ek}$  is an expression of force error, so this adaptive adjustment compensator can respond quickly to the change of the force error, that is to say, to the change of the environment. It is the reason why this expression is used as the compensator of impedance control [22].

$$\begin{aligned} q(t) &= \omega_p e(t) + \omega_d \dot{e}(t) \\ g(t) &= g_0 + \alpha_1 \int_0^t q(t) dt + \alpha_2 q(t) \\ k_p(t) &= k_{p0} + \beta_1 \int_0^t q(t) e(t) dt + \beta_2 q(t) e(t) \\ k_d(t) &= k_{d0} + \gamma_1 \int_0^t q(t) \dot{e}(t) dt + \gamma_2 q(t) \dot{e}(t) \end{aligned} \quad (12)$$

Where,  $\omega_p$  and  $\omega_d$  are the positive position and velocity weighting factors respectively;  $\alpha_1, \beta_1, \gamma_1$  are the positive integral adaptation gains respectively;  $\alpha_2, \beta_2, \gamma_2$  are the positive or zero proportional adaptation gains; moreover,  $k_{d0}, k_{p0}, g_0$  are the initial values and equal to zero. Since the actual contact force is measured by the force sensor is often a noisy signal, therefore the derivative of the force error is unsatisfying. To solve this problem,  $\dot{e}(t)$  is replaced by  $-k_e \dot{x}(t)$  in equations (11) and (12), and  $k_p$  are positive constants. Finally the modified expressions of the compensator are given by:

$$\begin{aligned} \Delta x_k &= g(t) + k_p(t)e(t) - k_v(t)\dot{x}(t) \\ q(t) &= \omega_p e(t) - \omega_v \dot{x}(t) \\ g(t) &= g_0 + \alpha_1 \int_0^t q(t) dt - \sigma_1 \int_0^t g(t) dt \\ k_p(t) &= k_{p0} + \beta_1 \int_0^t q(t) e(t) dt - \sigma_2 \int_0^t k_p(t) dt \\ k_d(t) &= k_{v0} - \lambda_1 \int_0^t q(t) \dot{x}(t) dt - \sigma_3 \int_0^t k_v(t) dt \end{aligned} \quad (13)$$

Where  $\lambda_1 = \gamma_1 k_e$ ,  $\omega_v = \omega_d k_e$  and  $\sigma_1, \sigma_2, \sigma_3$  are small positive constants. The Cartesian and joint coordinate systems are built, as shown in Fig. 6, where O0 is Cartesian coordinate system and O1 ·O2 ·O3 ·O4 are the coordinate system of each joint, the kinematics equation of the three-DOF finger is expressed as:

$$\begin{aligned} A &= A_1 A_2 A_3 A_4 A_5 \Rightarrow \\ A_1 &= \begin{bmatrix} 1 & 0 & 0 & 0 \\ 0 & \cos \theta_1 & -\sin \theta_1 & L_0 \\ 0 & \sin \theta_1 & \cos \theta_1 & 0 \\ 0 & 0 & 0 & 1 \end{bmatrix} & A_2 &= \begin{bmatrix} \cos \theta_2 & -\sin \theta_2 & 0 & 0 \\ \sin \theta_2 & \cos \theta_2 & 0 & L_1 \\ 0 & 0 & 1 & 0 \\ 0 & 0 & 0 & 1 \end{bmatrix} \\ A_3 &= \begin{bmatrix} \cos \theta_3 & -\sin \theta_3 & 0 & 0 \\ \sin \theta_3 & \cos \theta_3 & 0 & L_2 \\ 0 & 0 & 1 & 0 \\ 0 & 0 & 0 & 1 \end{bmatrix} & A_4 &= \begin{bmatrix} \cos \theta_4 & -\sin \theta_4 & 0 & 0 \\ \sin \theta_4 & \cos \theta_4 & 0 & L_3 \\ 0 & 0 & 1 & 0 \\ 0 & 0 & 0 & 1 \end{bmatrix} \\ A_5 &= \begin{bmatrix} 1 & 0 & 0 & 0 \\ 0 & 1 & 0 & L_4 \\ 0 & 0 & 1 & 0 \\ 0 & 0 & 0 & 1 \end{bmatrix} & A &= \begin{bmatrix} n_x & O_x & a_x & x \\ n_y & O_y & a_y & y \\ n_z & O_z & a_z & z \\ 0 & 0 & 0 & 1 \end{bmatrix} \end{aligned} \quad (14)$$

where  $x$ ,  $y$  and  $z$  are the coordinate values of the fingertip in Cartesian coordinate system. The following equations can be obtained from Eq. (14):

$$\begin{cases} -y \sin \theta_1 + z \cos \theta_1 + L_0 \sin \theta_1 = 0 \\ w_1^2 + (w_2 - L_2)^2 - 2L_3(-w_1 \sin \theta_3 + (w_2 - L_2) \cos \theta_3) + L_3^2 = L_4^2 \\ (q_2 - L_1)^2 + q_1^2 - 2((q_2 - L_1) \cos \theta_2 - q_1 \sin \theta_2)L_2 + L_2^2 = L_4^2 + L_3^2 + 2L_4 L_3 \cos \theta_4 \\ m_1 \cos \theta_4 + m_2 \sin \theta_4 - L_3 \sin \theta_4 = 0 \\ \begin{cases} q_1 = x \\ q_2 = y \cos \theta_1 + z \sin \theta_1 - L_1 \cos \theta_1 \\ w_1 = q_1 \cos \theta_2 + q_2 \sin \theta_2 - L_1 \sin \theta_2 \\ w_2 = -q_1 \sin \theta_2 + q_2 \cos \theta_2 - L_1 \cos \theta_2 \\ m_1 = w_1 \cos \theta_3 + w_2 \sin \theta_3 - L_2 \sin \theta_3 \\ m_2 = -w_1 \sin \theta_3 + w_2 \cos \theta_3 - L_2 \cos \theta_3 \end{cases} \end{cases} \Rightarrow \quad (15)$$

In addition, there is relationship between  $\theta_3$  and  $\theta_4$  due to the coupled structure, as expressed below.

$$\begin{aligned} L &= \sqrt{r_p^2 + L_3^2 - 2r_p L_3 \cos \theta_3} \\ \alpha &= ar \cos \left( \frac{r_1^2 + L^2 - L_g^2}{2r_1 L} \right) \\ \beta &= \alpha - ar \cos \left( \frac{L_3^2 + L^2 - r_p^2}{2LL_3} \right) \\ \theta_4 &= \pi - \rho - \beta \end{aligned} \quad (16)$$

Where  $\rho = 1.52$ ,  $r_p = 4mm$ ,  $L_g = 27mm$ ,  $r_1 = 6.2mm$ . In order to control the position of the robot finger accurately, it is necessary to get the relationship between the joint angular displacements and the tendon displacements. Due to the particular design and neglecting the tendon elasticity, the relationship can be expressed as:

$$\Delta l = R^T \Delta \theta \quad (17)$$

Where  $R$  is defined in Equation (3).

6 RESULTS

Simulation of the thumb exoskeleton is built in MATLAB with sample time of 0.001 s. The impedance parameters and the adaptive parameters are given by:

$$M_d = \begin{bmatrix} 200 & 0 & 0 \\ 0 & 200 & 0 \\ 0 & 0 & 200 \end{bmatrix} kg$$

$$K_d = \begin{bmatrix} 100 & 0 & 0 \\ 0 & 100 & 0 \\ 0 & 0 & 100 \end{bmatrix} N/m$$

$$B_d = \begin{bmatrix} 3000 & 0 & 0 \\ 0 & 3000 & 0 \\ 0 & 0 & 3000 \end{bmatrix} N/(m/s)$$

$$\sigma_1 = 0.001, \sigma_2 = \sigma_3 = 0.09, \alpha_1 = \beta_1 = \lambda_1 = 0.01, \omega_p = 0.27, \omega_v = 0.25 \quad (18)$$

In the free space, the finger motion is controlled by the position controller. The final-desired angular displacements of the joints are  $[0, -0.17, -1.25]T$ . Then the module controller controls the finger motion according to the desired trajectories. Three rehabilitation approaches taken into account based on patients' feedback will be discussed in the following. This is completely clear that the robotic system which provides assistance regardless of the actual performance of the patient will not be effective.

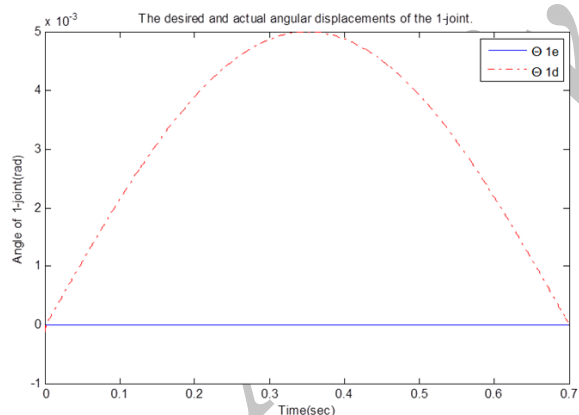


Fig. 6 Desired and actual angular displacements of the joint 1

As it was previously mentioned, the motion-based therapy has better results in improving the patient's movements compared to the traditional treatment. So, the rehabilitation system presented in this research gives the patient more assistance only when the person needs help. Hence the effectiveness and efficiency of the suggested approach will be far more. In the proposed rehabilitation system, the auxiliary controller provides assistance based on the actual performance of the patient. In other words, the individual will receive assistance when his finger position is beyond a

specified and acceptable border or the feedback system receives patient's help request. If the patient is in the final stages of rehabilitation, thumb motion will be faster and the patient needs less force applied by exoskeleton. Hence, the power of joints for performing the motion will gradually increase until the final value of  $[-1.2 \ 3 \ 0.2]N$  became stable. Moreover, the finger reaches the desired angle in 0.7s. Figures 6 and 7 illustrate the results of angular control simulation of three joints of the thumb. As it is seen, the controller could follow the desired angles with the precision of more than  $10^{-2}$  rad. The error was due to the friction between parts and uncertainty of some parameters. So, on the whole, the results are satisfactory considering the controller performance.

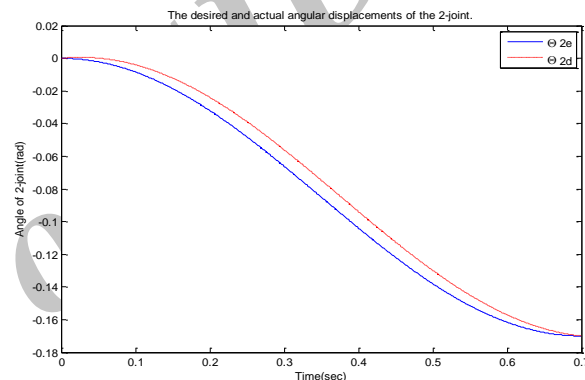


Fig. 7 Desired and actual angular displacements of the joint 2

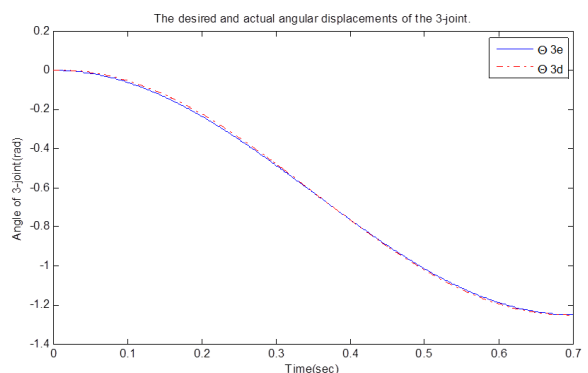


Fig. 8 Desired and actual angular displacements of the joint 1

Figure 9 shows the force tracking by exoskeleton joints. It is observed that the force tracking error has become zero by the controller without any overshoots. Moreover, as it was mentioned before, the fast thumb motion mode tries to make the patient to apply more force or in other words, the least amount of help is provided. Then, the applied force in this mode will be less than two other modes. Figs. 10 and 11 show the

three dimensional and two dimensional desired and actual trajectory of the thumb motion. As it is observed, the finger-tip coordination has transmitted from  $[0 \ 0.113 \ 0]$  to  $[0.0517 \ 0.0807 \ 0]$ . Fig. 12 shows the trajectory tracking error by the exoskeleton in Desecration coordinate and indicates the desired performance of controller system since the maximum tracking error in Desecration coordinate was  $10^{-3}$ .

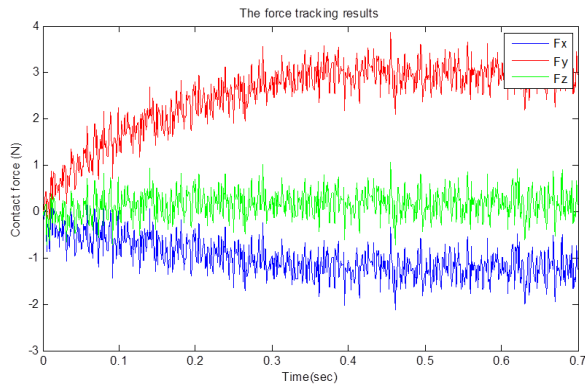


Fig. 9 Thumb force tracking

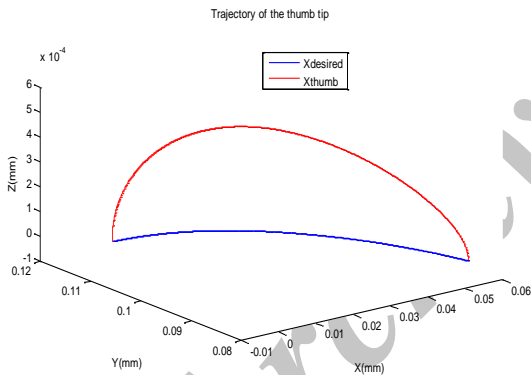


Fig. 10 Three dimensional finger-tip trajectory in desecration coordinate

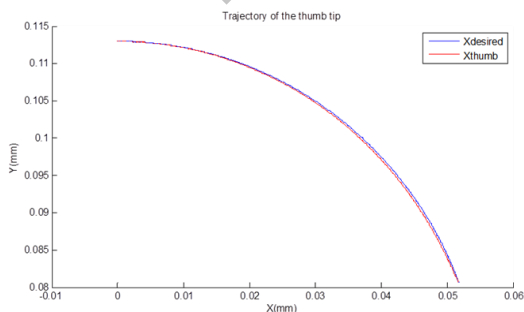


Fig. 11 Two dimensional finger-tip trajectory in desecration coordinate

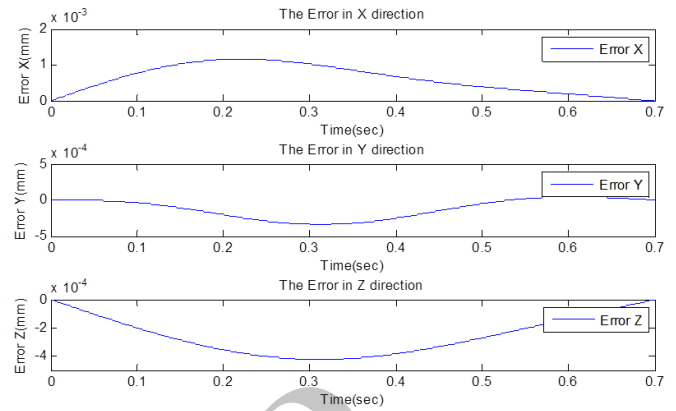


Fig. 12 Tracking error of Exoskeleton in Desecration coordinate

If patients suffer by moving the fingers or need more help for moving his finger, the motion of the finger will be slower and consequently more force will be applied by the exoskeleton. Hence, it is tried to reduce the pain intensity and perform the motions correctly. At this stage of rehabilitation, the applied force on the joints will increase to the maximum value of  $[-1.5 \ 3.9 \ 0.26]N$ . It should be mentioned here, that the ratio of applied force is more than the fast motion. Then, considering the patients need for more applied force and slower motion of the finger, it takes 0.91 s for the thumb to reach the desired angle. Figures 13 to 15 show the simulation of angle controlling in three finger joints with average motion. The controller's tracking is satisfactory and tracking errors are negligible. Inertia of the mechanical pieces could be a source of error, where this inertia caused to system dilation, obviously in joint 2.

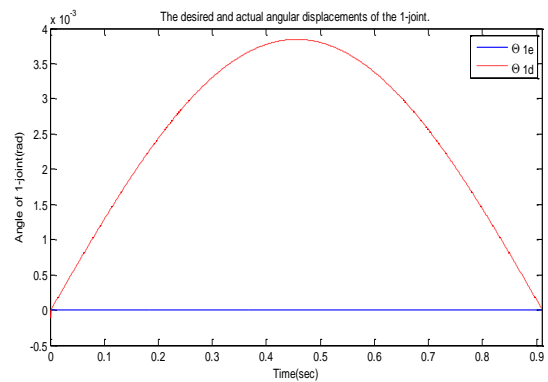


Fig. 13 Desired and actual angular displacements of joint 1



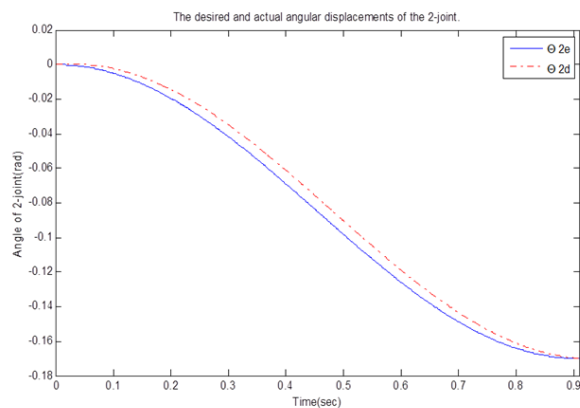


Fig. 14 Desired and actual angular displacements of joint 2

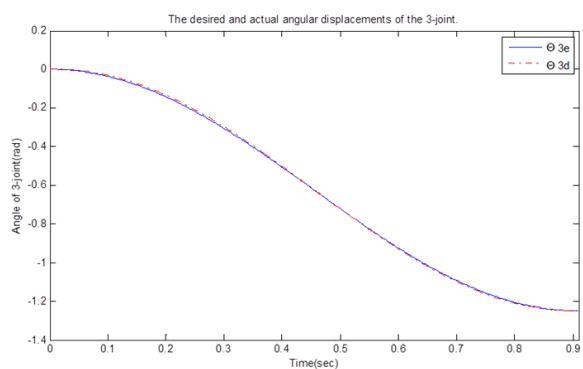


Fig. 15 Desired and actual angular displacements of joint 2

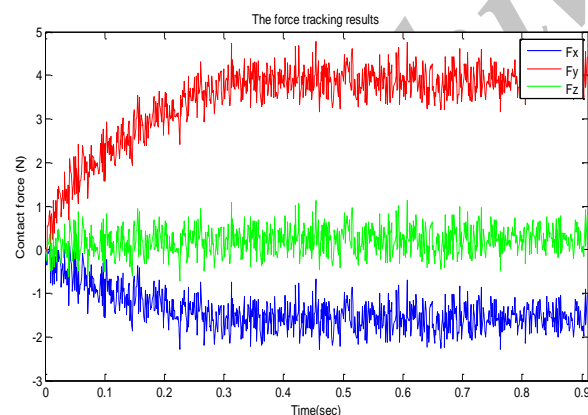


Fig. 16 Thumb force tracking

Fig. 16 shows the force tracking by exoskeleton joints. It is observed that the force tracking error has become zero after 0.15 s by the controller without any overshoots. Moreover, as it was stated before, the applied force in this mode will be more than fast modes. Figs. 17 and 18 show the three dimensional and two dimensional desired and actual trajectory of the thumb motion. As it is observed, the finger-tip coordination has transmitted from  $[0 \ 0.113 \ 0]$  to

$[0.0517 \ 0.0807 \ 0]$ . Fig. 12 shows the trajectory tracking error of the exoskeleton in Desecration coordinate indicating the desired performance of controller system since the maximum tracking error in Desecration coordinate was  $10^{-3}$ .

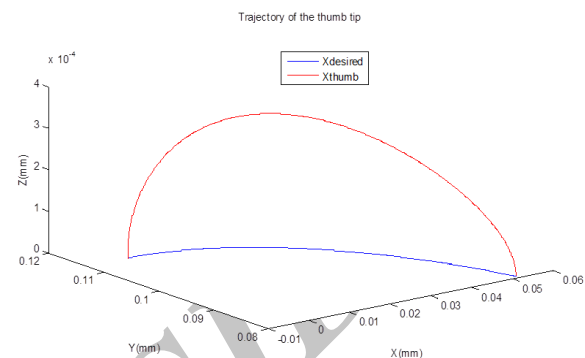


Fig. 17 Three dimensional finger-tip trajectory in desecration coordinate

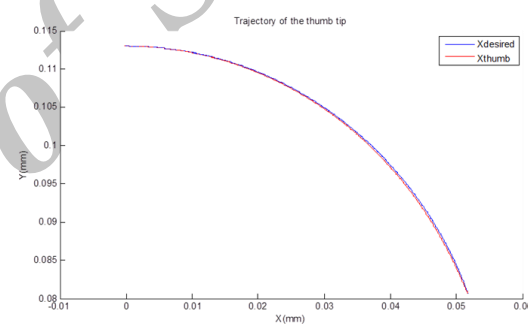


Fig. 18 Two dimensional finger-tip trajectory in desecration coordinate

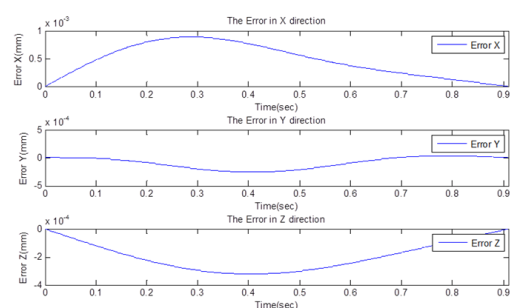


Fig. 19 Tracking error of Exoskeleton in Desecration coordinate

If the patient is in the first stages of rehabilitation, slower thumb motion is suggested since the patient cannot perform fast motion and do not have enough joint power for performing the motions. Moreover, the finger should move slowly to prevent suffering and pain. On the other hand, slowing down the motion will improve the precision. In this mode, finger reaches the final desired angle after 1.15s.

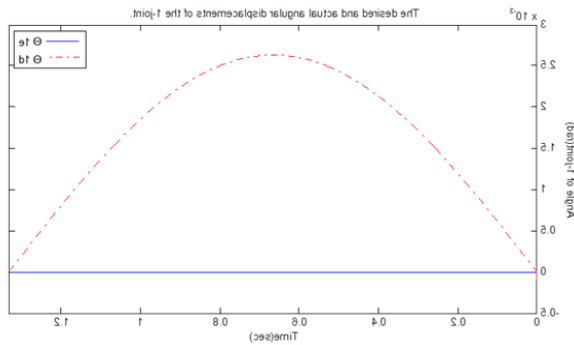


Fig. 20 Desired and actual angular displacements of joint 1

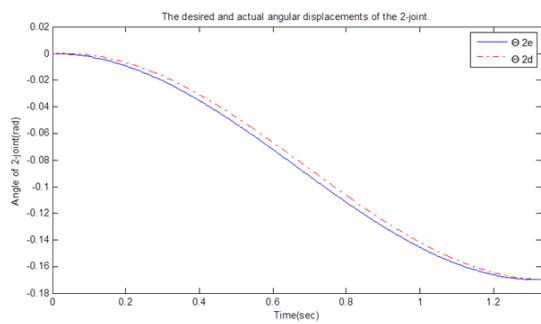


Fig. 21 Desired and actual angular displacements of joint 2

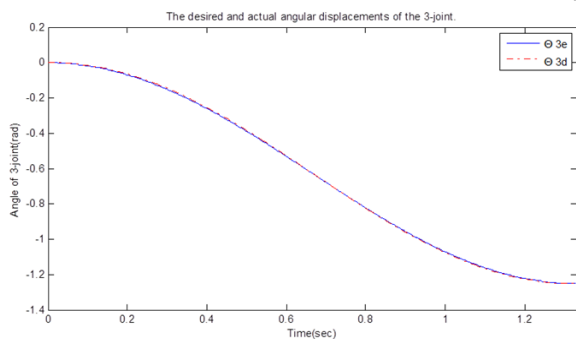


Fig. 22 Desired and actual angular displacements of joint 3

Figs. 20 to 22 illustrate the results of angular control simulation of three joints of the thumb. As it is seen, the controller could follow the desired angles with the precision of more than before. This will be due to the slow movement of the joints which compensates the system inertia since the mechanic system is naturally slow and as the motion become slower, the precision will be more. The results of simulation indicate the same. As it is seen in Fig. 18, the applied force in this DOF is more than the other two. So that the applied force on the joints reach the maximum value of

$[-2.28 \ 5.7 \ 0.38]N$  since more help is given to the patients. Figs. 24 and 25 show the three dimensional and two dimensional desired and actual trajectory of the thumb motion. The trajectories of three degrees of freedom are the same. Fig. 23 shows that the trajectory tracking error of the exoskeleton in Desecration coordinate has been reduced compared to the two other modes.

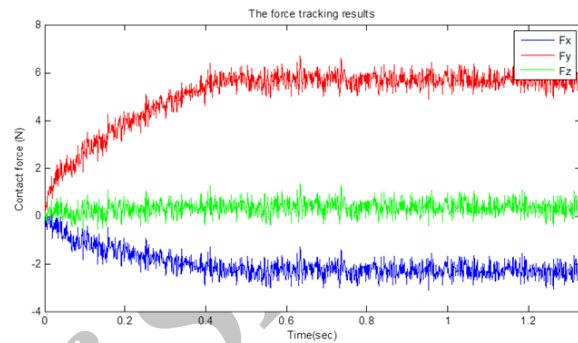


Fig. 23 Thumb force tracking

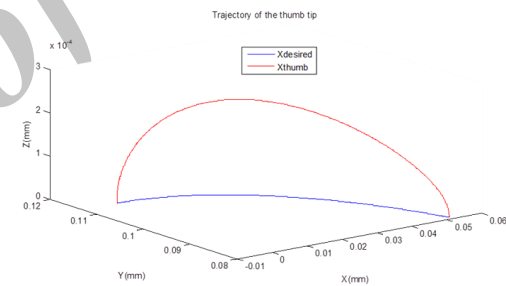


Fig. 24 Three dimensional finger-tip trajectory in desecration coordinate

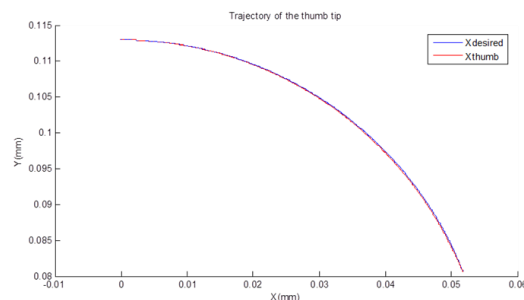
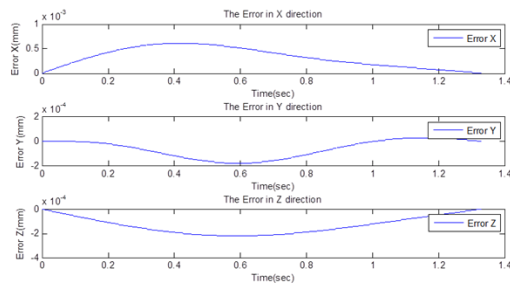


Fig. 25 Two dimensional finger-tip trajectory in desecration coordinate



**Fig. 26** Tracking error of Exoskeleton in Desecration coordinate

## 7 CONCLUSION

Stroke is the main cause of permanent disability of adults worldwide. Stroke often affects the upper limb motor control and lead to the creation of problems in carrying out daily activities. Every year many medical expenses are spent to regain upper limb motor ability of the patients. So, an exoskeleton of thumb finger was applied and analyzed for rehabilitation of patients affected by stroke. The study aimed to design a thumb exoskeleton in order to keep patients in the process of treatment, reducing therapists' intervention and get feedback from patients to improve the rehabilitation process and reduce the discomfort of patients during the course of treatment.

A three degree-of-freedom exoskeleton was designed and the mathematical equations were rewritten. Finally, the controller was modified based on patients' feedback. Moreover, the controller of the suggested system can be activated or deactivated. This advantage leads to application of robotic help when required. It should be mentioned that, in order to avoid too much pressure, a switch is provided for optimal force reactions so that the status changes slowly. Thumb exoskeleton was simulated in MATLAB.

The results of simulation indicated efficient and satisfactory performance of the exoskeleton. As it was found, the simulated exoskeleton had a proper tracking of desired trajectory. Moreover, the controller could track the trajectory without overshooting. These are the most important characteristic of a controller in the system to evaluate its performance, since overshooting in this process will cause shocks in finger motion while due to the sensitive nature of patient's condition, motions must be slow and performed without any shock.

Another advantage of this design was including patient feedback in rehabilitation. Therefore, the designed system had a variety of adaption capabilities with different rehabilitation courses. Also according to the ability to change the amount of applied force, it

facilitated the finger motion causing its reliability and returning the patients' self-confidence.

## REFERENCES

- [1] American Heart Association, Heart and Stroke Statistical Update, Available: <http://www.Americanheart.org/statistics/stroke.htm>, 2010.
- [2] Patten, C., Christine, E., Dairaghi, A., and Lum P., "Concurrent Neuromechanical and Functional Gains Following Upper-Extremity Power Training Post-Stroke", *J Neuroeng Rehabil*, Vol. 10, No. 1, 2013.
- [3] Albert, C., Lo, Peter, D., Guarino and et al., "Robot-Assisted Therapy for Long-Term Upper-Limb Impairment after Stroke", *New England Journal of Medicine*, Vol. 362, No. 19, 2010, pp. 1772-1783.
- [4] Michielsen, ME., Selles, RW., Vander Geest JN., Eckhardt, M., Yavuzer, G., Stam, HJ., Smits, M., Ribbers GM., and Bussmann, JB., "Motor Recovery and Cortical Reorganization after Mirror Therapy in Chronic Stroke Patients a Phase II Randomized Controlled Trial", *Neurorehabilitation and Neural Repair*, Vol. 25, No. 3, 2011, pp. 223-215.
- [5] Hayner, K., Gibson, G., and Giles, G. M., "Comparison of Constraint-Induced Movement Therapy and Bilateral Treatment of Equal Intensity in People with Chronic Upper-Extremity Dysfunction after Cerebrovascular Accident", *The American Journal of Occupational Therapy*, Vol. 64, No. 4, 2010, pp. 528-539.
- [6] Hammer, A. M., Lindmark, B., "Effects of Forced Use on Arm Function in the Subacute Phase after Stroke: A Randomized, Clinical Pilot Study", *Physical Therapy*, Vol. 89, No. 6, 2009, pp. 526-539.
- [7] Novak, D., Zihlerl, Z., Olensek, A., and Milavec, M., et al., "Psychophysiological Responses to Robotic Rehabilitation Tasks in Stroke", *IEEE Transactions on Neural Systems and Rehabilitation Engineering*, Vol. 18, No. 4, 2010, pp. 171-361.
- [8] Choi, H., Gordon, J., Kim, D., and Schweighofer, N., "An Adaptive Automated Robotic Task-Practice System for Rehabilitation of Arm Functions after Stroke", *IEEE Transactions on Robotics*, Vol. 25, No. 3, 2009, pp. 556-568.
- [9] Poli, P., Morone G., Rosati G., and Masiero S., "Robotic Technologies and Rehabilitation: New Tools for Stroke Patients' Therapy", *BioMed Research International*, 2013, pp. 153872.
- [10] Esmzade, R., and Khosrojerdi M., "Modeling and Control of the Exoskeleton for Rehabilitation of Shoulder, Elbow and Wrist Motions", *nineteenth Conference on Biomedical Engineering*, 2012.
- [11] Jamshidi, M., Rahmanzade, H., and Kaboudi, T., "Robotic Modeling for Rehabilitation of Arm and Knee Muscles", *First Conference of Rehabilitation Robotics*, 2012.
- [12] Abdolvahab, M., Bagheri H., Movahedian, M., Olyaei GR., Jalili, M., and Baghestani, AR., "The effect of constraint-induced therapy on Activity of Daily Living of adults hemiplegic patients", (in

- Persian), *Modern Rehabilitation*, Vol. 3. No. 1, 2, 2008, pp. 28-32.
- [13] Worsnopp, T. T., Peshkin, M. A., Colgate, J. E., and Kamper, D. G., "An actuated finger exoskeleton for hand rehabilitation following stroke", *Proceedings of the IEEE 10th International Conference on Rehabilitation Robotics*, Vol. 1, 2007.
- [14] Santos, V., Valero-Cuevas, F., "Reported Anatomical Variability Naturally leads to multimodal distributions of Denavit\_Hartenberg parameters for the human thumb", *IEEE Transactions on Biomedical Engineering*. Vol. 53, No. 2, 2006, pp. 155-63.
- [15] Abdallah, M. E., Platt, R., and Wampler, C. W., "Hargrave, B., Applied Joint-Space Torque and Stiffness Control of Tendon-Driven Fingers", In *Proceedings of the 10th IEEE-RAS International Conference on Humanoid Robots (Humanoids)*, Nashville, TN, USA, 6–8 December, 2010, pp. 74–79.
- [16] Borghesan, G., Palli, G., and Melchiorri, C., "Design of Tendon-Driven Robotic Fingers: Modeling and Control Issues", In *Proceedings of the IEEE International Conference on Robotics and Automation*, Anchorage, AK, USA, 3–7 May 2010, pp. 793–798.
- [17] Otadi, K., Hadian, MR., Olyaei, GR., Rasoulia, B., Emamdoost, S., Barikani, E., Torbatian, E., and Ghasemi, A., "The effect of modified constraint induced movement therapy on quality and amount of upper limb movements in chronic hemiplegic patients in comparison with traditional rehabilitation" (in Persian), *Modern Rehabilitation*, Vol. 6, No. 1, 2012, pp. 13-18.
- [18] Bagheri, H., Abdolvahab, M., Dehghan L., Jalili M., and Beheshti, S., Z., "The effect of task oriented training on upper extremity function in children with spastic diplegia 8-12 years old" (in Persian), *Modern Rehabilitation*, Vol. 3, No. 3, 2010, pp. 57-61.
- [19] Sung, HoCA, J., Yun-Hee, K., Sang-Hyun, CH., Jin-Hee, L., Ji-Won, P., and Yong-Hyun, K., "Cortical reorganization induced by task-oriented training in chronic hemiplegic stroke patients", *Neuroreport*, Vol. 14, No. 1, 2003, pp. 137-141.
- [20] Lu, E., Wang, R., Boger, Hebert, J, D., and Mihailidis, A., "Development of a rehabilitation robot: national differences in therapist practice", in *Rehabil. Eng. Assist. Technol. Soc.*, 2011.
- [21] Dovat, L., Lamercy, O., et al., "HandCARE: a cable-actuated rehabilitation system to train hand function after stroke", *IEEE Trans Neural Syst. Rehabil. Eng.*, Vol. 16, 2013, pp. 582-91.
- [22] Li, J. W., Bu, C. G., and Wang, L., "The application of Macro command in ADAMS in building the virtual prototype of cable drill", *Mach. Tool Hydraul.*, Vol. 39, 2011, pp. 150–153.